

UC Davis

UC Davis Previously Published Works

Title

TLR8 activation and inhibition by guanosine analogs in RNA: Importance of functional groups and chain length

Permalink

<https://escholarship.org/uc/item/2q21w729>

Journal

Bioorganic & Medicinal Chemistry, 26(1)

ISSN

0968-0896

Authors

Hu, Tiannan
Suter, Scott R
Mumbleau, Madeline M
[et al.](#)

Publication Date

2018

DOI

10.1016/j.bmc.2017.11.020

Peer reviewed



Published in final edited form as:

Bioorg Med Chem. 2018 January 01; 26(1): 77–83. doi:10.1016/j.bmc.2017.11.020.

TLR8 activation and inhibition by guanosine analogs in RNA: importance of functional groups and chain length

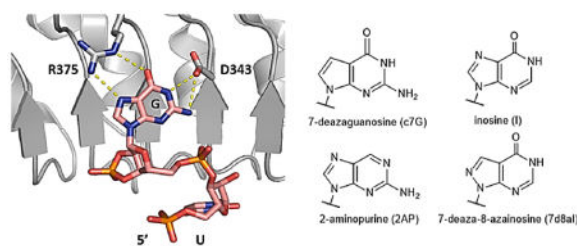
Tiannan Hu^a, Scott R. Suter^a, Madeline M. Mumbleau^a, and Peter A. Beal^{a,*}

^aDepartment of Chemistry, University of California, One Shields Ave, Davis, CA 95616

Abstract

Toll-like receptor 8 (TLR8) is an important component of the human innate immune system that recognizes single stranded RNA (ssRNA). Recent x-ray crystal structures of TLR8 bound to ssRNA revealed a previously unrecognized binding site for a 5'-UpG-3' dinucleotide. Here we use an atomic mutagenesis strategy coupled with a cellular TLR8 activation assay to probe the importance of specific functional groups present on the guanine base in RNA-mediated receptor agonism and antagonism. Results from RNA analogs containing 7-deazaguanosine, 2-aminopurine and inosine confirm the importance of guanine N7, O6 and N2, respectively, in TLR8 activation. Nevertheless, these RNAs each retained TLR8 antagonism activity. RNA containing 7-deaza-8-azainosine (7d8aI) was prepared from a novel phosphoramidite and found to be a weaker TLR8 activator than guanosine-containing RNA. However, 7d8aI-containing RNA also retained TLR8 antagonism activity indicating that removal of multiple TLR8 H-bonding sites on guanine is insufficient for blocking TLR8 antagonism by guanine-containing RNA. We also identified an oligoribonucleotide length dependence on both TLR8 activation and antagonism. These studies extend our understanding of the effects of nucleobase modification on immune stimulation and will inform the design of novel RNA-based therapeutics.

Graphical Abstract



Keywords

TLR8; RNA; Guanosine; Antagonism; Immune response

*Corresponding author. Tel.: +1-530-752-4280; fax: +0-000-000-0000; pabeal@ucdavis.edu.

Publisher's Disclaimer: This is a PDF file of an unedited manuscript that has been accepted for publication. As a service to our customers we are providing this early version of the manuscript. The manuscript will undergo copyediting, typesetting, and review of the resulting proof before it is published in its final citable form. Please note that during the production process errors may be discovered which could affect the content, and all legal disclaimers that apply to the journal pertain.

Introduction

Toll-like receptors constitute a family of pattern recognition receptors that recognize molecules widely shared by pathogens.¹ These receptors play important roles in the innate immune system, which serves as a key defense against infection in humans.¹ However, over activation of TLRs is often seen in various types of autoimmune disease, such as systematic lupus erythematosus (SLE), rheumatoid arthritis (RA) and multiple sclerosis (MS).² TLRs also play important roles in the failure of many clinical treatments, such as graft vs. host disease (GvHD)³ and in immune responses to nucleic acid-based therapeutics.⁴ Thus, understanding ligand recognition by TLRs and TLR receptor activation is important for future drug development.

Toll-like receptor 8 (TLR8) is an endosomal immune receptor that recognizes single stranded RNA (ssRNA), and can recognize ssRNA viruses such as Influenza, Sendai, and Coxsackie B viruses.⁵ TLR8 binding to viral RNA recruits MyD88 and leads to activation of the transcription factor NF- κ B and an antiviral response.⁶ In addition to detecting viral ssRNA, TLR8 also plays a key role in the development of autoimmune diseases by recognizing high levels of ssRNA in serum.⁷ Investigators have shown that the TLR8-mediated immune response is crucial in the development of fetal congenital heart block (CHB) with maternal autoantibodies,⁸ while the activation of TLR8 is relevant to the onset and progress of RA and MS.² However, the study of TLR8 and its clinical significance is under explored compared to other TLRs. This is likely due to the fact that TLR8 functions differently in mice and humans, and both TLR8 and TLR7 recognize ssRNA as a pathogen-associated molecular pattern (PAMP), making it difficult to interpret data from primary immune cells, such as peripheral blood mononuclear cells (PBMCs), where both receptors are expressed.

Recent structural studies of TLR8 and its complexes with different ligands have advanced our understanding of the mechanism of TLR8 activation by RNA. In 2015, Tanji et al. solved the first x-ray crystal structure of TLR8 bound to ssRNA.⁹ Surprisingly, these authors did not observe an intact ssRNA chain in the structure. Rather, TLR8 appeared to bind RNA fragments, possibly arising from degradation of the ssRNA during crystallization (Figure 1). In the structure, uridine is bound to one site in the protein, whereas a second binding site is occupied by a 5'-UpG-3' dinucleotide (Figure 1a). Uridine was found at a location on the receptor previously identified as a small molecule binding site from structures of TLR8 bound to low molecular weight agonists (e.g. R848).¹⁰ However, the UpG-binding site was previously unknown. Moreover, the binding affinity of TLR8 for uridine is 10 times lower in the absence of UpG. Also activation of TLR8 could only be achieved by co-incubating uridine and the UpG-containing oligonucleotide. Mutagenesis studies around the second binding site also suggested a crucial role for this site in the activation of TLR8 by RNA. Together, these results highlight the importance of the UpG binding site in the activation of TLR8 by ssRNA.

As a part of our ongoing efforts to explore the effect of nucleobase analogs on immune responses induced by RNA,^{11, 12} we endeavored to define structure-activity relationships for RNA containing guanine analogs binding to TLR8 (Figure 1). We focused on guanine since

the U in the UpG dinucleotide bound in the second site is found in different conformations in structures of TLR8-RNA complexes, whereas the position of the G is always fixed.⁹ There have been other studies that describe the effects of guanosine derivatives on TLR8 activation by RNA. Sioud et al. reported 2'-OMe modification of guanosine can suppress TLR8 activation by ssRNA.¹³ Lan et al. reported 7-deazaguanosine-containing RNA is a moderate agonist of TLR8 while strongly activating toward TLR7.¹⁴ Sarvestani et al. reported inosine-containing RNA is a potential agonist of TLR7/8.¹⁵ However, no systematic study of how different functional groups on guanosine specifically affect the TLR8 response has been reported. Moreover, previous studies using PBMCs often cannot fully distinguish a TLR8 response from a TLR7 response since both receptors are expressed on these cells.

The strategy we chose to follow is an “atomic mutagenesis¹⁶” approach using RNA-containing nucleoside analogs. This was achieved by chemical synthesis of the ssRNA incorporating different analogs that alter specific functional groups of the guanine base. By testing the TLR8 response of these modified ssRNA strands, we were able to define the significance of each functional group to the TLR8 response. We also designed a novel guanosine analog and tested the TLR8 response of this nucleobase modification when incorporated into RNA.

Results and Discussion

We first tested the TLR8 response of 20-mer ssRNAs (Table 1. Oligonucleotide sequences used in the study) with different amounts of the UpG motif (Figure 2). In the crystal structure, UpG was observed as the ligand of TLR8 in the second binding site, and several reports have also indicated its importance in the sequence of TLR8 activating ssRNAs.^{17, 18} To this end, we designed a specific sequence with five 5'-CUGU-3' repeats wherein each G can be replaced with guanosine analogs or C as a negative control. The length of these test sequences was set to 20 nt to mimic the effect of siRNAs on TLR8, which have been reported to be TLR8 stimulatory.¹⁹ These sequences were also designed to minimize self-complementarity to minimize possible effects of RNA secondary structure on TLR8 response. To be specific to TLR8, HEK 293 cells that stably express only TLR8 were used in this study. Upon activation of TLR8, the NF- κ B signaling pathway is triggered in these cells, causing the expression of the reporter enzyme secreted alkaline phosphatase (SEAP).

By testing different oligonucleotides that vary the number of UpG motifs and their location relative to the 5' or 3' end, we found that TLR8 activation is positively correlated with the number of UpGs present in this 20-mer sequence, regardless of their relative positions within the sequence (Figure 2). At a concentration of 5 μ M, at least four UpGs are required in the 20-mer sequence to elicit a strong TLR8 activation in this assay. Hence, we chose the G5 oligonucleotide as the starting sequence to study the effect of guanosine modifications on the TLR8 response.

Next, we tested the effect of guanosine modifications on the TLR8 response. We substituted all Gs in G5 with inosine, 2-aminopurine or 7-deazaguanosine, respectively (Table 1, Figure 1).

We first tested the effect of functional groups on TLR8 activation. From the crystal structure of TLR8 bound to RNA (Figure 1), guanine interacts with TLR8 through four hydrogen bond donor-acceptor pairs: N7/R375, O6/R375, N1/D343 and N2/D343. We incorporated inosine to remove the interaction between N2 and D343, 2-aminopurine to remove both N1/D343 and O6/R375, and 7-deazaguanosine to remove N7/R375. The results show that while maintaining some agonistic activity, the substitution of G with inosine, 2-aminopurine, and 7-deazaguanosine each substantially decreased the agonistic activity of G5, to an extent similar to when G is replaced by adenosine (Figure 3). Together with the x-ray crystal structure and mutagenesis reported earlier,⁹ these results emphasize the importance of all four hydrogen bonding interactions to guanine for robust TLR8 activation.

It is well known that competitive binding of non-activating ligand could lead to an antagonistic effect on the receptor. We also tested the antagonism of RNAs with guanosine analogs on TLR8, using G5 as the activator. The results show that ssRNAs with Gs substituted into inosine, 2-aminopurine or 7-deazaguanosine each can antagonize TLR8 activation by G5, with c7G5 being the strongest antagonist (Figure 3). No significant cytotoxicity was observed (Figure S1), indicating that the antagonist effect shown above was not a misinterpretation of cell death. It is worth noting that removal of the N7/R375 interaction dramatically switched guanosine from an agonist into an antagonist, suggesting the crucial role of N7/R375 in the activation of TLR8.

It has been reported that 2'-OMe modified oligonucleotides can antagonize TLR8 activation elicited by RNA, but not by a small molecule agonist such as R848.²⁰ We also observed a similar phenomenon with c7G5 (Figure 4). This suggests that the antagonism of c7G5 is most likely through the competitive binding to the second binding site, which is only required in the activation of TLR8 by RNA. We also observed a dependence of chain length in the antagonism of c7G containing ssRNAs (Figure 5). The antagonism of 7-deazaG containing RNA is stronger with a longer chain length, given the same total concentration of Uc7G motifs. The 4-mer 5'-CUc7GU-3' is a much less effective antagonist than is the 20 mer c7G5. Interestingly, another recent study on 2'-OMe containing RNA from Schmitt et al. observed similar trend of chain length on antagonism.²¹ Together, the ssRNA length effects on receptor activation and inhibition suggest additional contacts made outside the dinucleotide binding site contribute to the effects of RNA on TLR8 function. It is possible that TLR8 binds a UpG-rich RNA longer than a dinucleotide at its second binding site but the additional interactions are too weak to be observed in the crystal structure.

In the field of RNA therapeutics, although sometimes it is beneficial for the RNA to be intrinsically immune-active or immune-suppressive,²² immune responses are generally considered as unwanted off-target effects. Strong activation of innate immune receptors such as TLRs by siRNA contributes to adverse effects.²³ On the other hand, intrinsically immune-suppressive RNA that inhibit TLR activation could render a patient vulnerable to infection.²⁴ Thus, it would be ideal to develop new chemical modifications on RNA that are completely orthogonal to immune receptors like TLR8. Based on the structural studies and our previous results, we anticipated that 7-deaza-8-azainosine (7d8aI, the ribonucleoside of allopurinol) (Figure 6a), which has one less hydrogen bonding interaction than either I or c7G, could be

a poor TLR8 agonist and could show even weaker antagonism than I or c7G when incorporated into RNA.

The synthesis and incorporation of 7d8aI into RNA was achieved by standard solid phase synthesis via phosphoramidite chemistry (Scheme 1). In our synthesis, 7-deaza-8-azaadenine was first glycosylated via Vorbruggen glycosylation.²⁵ After deprotection, 7-deaza-8-azaadenosine is then converted into 7-deaza-8-azainosine by the enzyme adenosine deaminase (ADA). This reaction benefits from the fact that ADA can catalyze the deamination reaction of 8-azaadenosine at a faster rate than on adenosine.²⁶ The protection of the 5' and 2' hydroxyls by DMTr and TBDMS, respectively was followed by phosphoramidite formation. The 7d8aI analog was incorporated into RNA by standard solid phase coupling.

As predicted from the crystal structure and SAR studies, 7d8aI indeed showed decreased agonistic activity against TLR8 compared with guanosine (Figure 6b). While it also showed less antagonism against TLR8 compared with c7G, its effect is similar to that of inosine (Figure 6c). Again, no cytotoxicity was observed with these oligos under these conditions (Figure S1). This indicates that additional modification strategies, such as the addition of sterically blocking groups, may be required to remove completely the TLR8 antagonism of RNA containing guanosine analogs. We also carried out a thermal melting temperature (T_m) analysis to evaluate the base pairing stability of this new nucleobase modification. When compared with inosine, 7d8aI showed better selectivity in base pairing with cytosine in a 5'-UX-3' sequence context (Figure S2). This property of 7d8aI holds potential in applications such as sequence detection by hybridization or elimination of off-target effects in siRNA. Further evaluation of this new guanosine modification is currently underway in our lab.

Conclusion

Using synthetic guanosine analogs, we carried out a systematic structure-activity relationship study of the guanosine interaction with TLR8. Our experiments showed the importance of the UpG motif in the activation of TLR8 by ssRNA. We also showed that certain modifications of guanosine such as 7-deazaguanosine (c7G) could antagonize the activation of TLR8 by UpG-containing RNA, but could not antagonize TLR8 activation by R848. There is also a minimum length requirement on c7G containing oligonucleotide for the antagonistic effect. We then synthesized and incorporated 7-deaza-8-azainosine (7d8aI) into ssRNA that showed neither strong activation nor antagonism to TLR8 (Figure 7). The information revealed by these analogs not only supported findings from recently reported x-ray crystal structures, but also provided new insight into the mechanism of TLR8 recognition and activation by ssRNA. This information will inform the design of new guanosine modifications that have unique TLR8 activation/inhibition profiles, which could have potential in the development of therapeutic modulators of the innate immune system.

Experimental

1. Materials

1.1 General Materials—All RNA oligos except for 7d8aI5 were purchased from GE Dharmacon Inc., and were purified by polyacrylamide gel electrophoresis and desalted by SEP-PAK. RNA containing 7d8aI was synthesized by procedures described below. The concentration of all RNAs were determined by UV absorbance at 260 nm using a NanoDrop™ instrument. HEK293-TLR8 cells were purchased from Novusbio Inc., together with Secreted Alkaline Phosphatase Reporter Assay Kit. DOTAP transfection reagent were purchased from Sigma. The reagents used in synthesis were either purchased from ThermoFisher or Sigma.

1.2 Synthesis of 7-deaza-8-azainosine phosphoramidite

4-Amino-1-(β-D-ribofuranosyl)-1H-pyrazolo[3,4-d]pyrimidine (2): Previously prepared compound (1)²⁵ was added to a flame dried flask (3.34 g, 5.76 mmol) and dried overnight, *in vacuo*. The next day, a 33% methyl amine solution in ethanol (40 mL) was added to the flask and allowed to stir over 24 h. The reaction was then concentrated to a slurry under reduced pressure, and 300 mL diethyl ether was added to the flask to suspend the product. The mixture was then filtered, providing a pure white solid. (97% yield, 5.59 mmol) ¹H NMR (CD₃OD, 600 MHz): δ (ppm) 8.18 (s, 1H), 8.12 (s, 1H), 6.235 (d, 1H), 4.73 (t, 1H) 4.42 (t, 1H) 4.10 (m, 1H) 3.79(dd, 1H) 3.65(dd 1H). ¹³C NMR (CD₃OD, 150 MHz): δ (ppm) 158.5, 155.47, 153.47,133.05, 100.92, 85.58, 73.94, 71.25, 62.61. ESIHRMS (m/z): calcd for C₁₀H₁₄N₅O₄ [M+H]⁺ 268.1046, obsd 268.1033.

1-(β-D-Ribofuranosyl)-1H-pyrazolo[3,4-d]pyrimidin-4(5H)-one (3): To a 50 mL Falcon tube, (2) was added (0.5 g, 1.86 mmol) and suspended in 10 mL of NaHPO₃ buffer (0.66 mM, pH 7.4). Adenosine Deaminase (300μg, Sigma-Aldrich) was then added to the solution and the Falcon tube was allowed to rock on an orbital shaker for 6 h. After 6 h, the solution turned clear and the reaction was analyzed using thin layer chromatography to reveal complete conversion to a new product. The reaction was filtered through a pad of Celite with ethanol and concentrated via a rotary evaporator. Once concentrated, the reaction product was recrystallized in ethanol to offer a pure white powder, which was filtered and dried overnight to yield the target compound (99% yield, 0.5 g, 1.85 mmol). ¹H NMR (CD₃OD, 600 MHz): δ (ppm) 8.12(s, 1H), 8.06(s, 1H), 6.265 (d, 1H), 4.68 (t, 1H), 4.44(t, 2H), 4.10 (m, 1H), 4.10 (m, 1H), 3.79(dd, 1H), 3.65(dd, 1H). ¹³C NMR (CD₃OD, 150 MHz): δ (ppm) 144.6, 136.7, 116.56, 56.15, 12.17, 127.2, 126.5, 49.4. ESIHRMS (m/z): calcd for C₁₀H₁₃N₄O₅ [M-H]⁻ 269.0886, obsd 269.0871.

1-(β-D-Ribofuranosyl)-5'-O-(4,4'-dimethoxytrityl)-1H-pyrazolo[3,4-d]pyrimidin-4(5H)-one (4): Compound (3) (100 mg, 0.373 mmol) was dried *in vacuo* overnight. Pyridine (2 mL) was then added to (3) and stirred in an ice bath. Silver nitrate, crushed to a fine powder and dried *in vacuo* overnight, was then added to the flask (69.4 mg, 0.410 mmol). Finally, dimethoxytrityl chloride was added to the flask (138 mg, 0.410 mmol). Stirring occurred on ice for 15 min, and then allowed to stir at 25 °C for 24 h. After 24 h, the solution was diluted in ethyl acetate and filtered through a pad of Celite. The

filtrate was evaporated to remove pyridine, resuspended in 10 mL ethyl acetate, and washed using 10% saturated sodium bicarbonate solution (2x) and brine. The organic layer was then dried over sodium sulfate. Flash column chromatography (4% methanol/dichloromethane) afforded the product (**4**) (131 mg, 64% yield) as a white foam. ¹H NMR (CD₃OD, 600 MHz): δ (ppm) 8.06 (s, 1H), 8.05 (s, 1H), 7.385 (d, J = 7.0 Hz, 3H), 7.26 (m, 6H), 7.14 (d, 4H), 6.32 (d, J = 2.9 Hz, 2H), 4.79 (d, J = 5Hz, 1H), 4.6 (t, J = 5Hz, 1H), 4.18 (m, 2H), 3.72 (s, 6H), 3.27 (dd, J = 10.3, 3.2 Hz, 1H), 3.18 (dd, J = 10, 5.9 Hz, 1H) ¹³C NMR (CD₃OD, 150 MHz): δ (ppm) 158.66, 158.54, 153.34, 147.55, 145.11, 135.96, 135.85, 135.16, 129.85, 127.95, 127.14, 126.17, 112.47, 106.38, 89.03, 85.86, 83.56, 73.83, 71.34, 64.07. ESIHRMS (m/z): calcd for C₃₁H₂₉N₄O₇ [M-H]⁻ 569.2036, obsd 569.2030.

1-(β-D-Ribofuranosyl)-5'-O-(4,4'-dimethoxytrityl)-2'-O-(t-butyl dimethylsilyl)-1H-pyrazolo[3,4-d]pyrimidin-4(5H)-one (5): Compound (**4**) (949 mg, 1.66 mmol) was dried *in vacuo* overnight. Pyridine (1.2 mL 15.2 mmol) were added to the solution, followed by anhydrous THF (12 mL). The reaction was the stirred, and finely powdered and dried silver nitrate was added to the reaction and allowed to stir for an additional 15 min, at which time the solution became cloudy. Finally, tert-butyl dimethyl silyl chloride was added to the flask (324 mg, 2.16 mmol) and the solution stirred for 24 h at room temperature. After 24 h, the reaction was filtered through a pad of Celite using ethyl acetate (10 mL) and extracted with saturated sodium bicarbonate (2x) and brine. The organic layer was dried over sodium sulfate. Flash column chromatography (50% ethyl acetate/hexanes) afforded 364 mg (31 % yield) of the 2' protected compound (**5**). ¹H NMR (CD₂Cl₂, 600 MHz): δ (ppm) 8.14 (s, 1H), 8.0 (s, 1H), 7.49 (d, J = 7.0 Hz, 2H), 7.36 (m, 5H), 7.29 (m, 4H), 6.79 (m, 2H) 6.28 (d, J = 5.3 Hz, 1H), 5.1 (t, J = 5Hz, 1H), 4.6 (m, 1H), 4.18 (m, 1H), 3.77 (s, 6H), 3.36 (dd, J = 10.6, 4.7 Hz, 1H), 3.15 (dd, J = 10.6, 4.7Hz, 1H) ¹³C NMR (CD₂Cl₂, 150 MHz): δ (ppm) 158.53, 158.54, 153.55, 146.68, 145.06, 136.07, 135.78, 130.10, 128.16, 127.70, 126.60, 112.98, 106.70, 88.46, 86.16, 84.20, 74.88, 71.95, 64.01, 25.33, 17.79, -5.31, -5.43. ESIHRMS (m/z): calcd for C₃₇H₄₃N₄O₇Si [M-H]⁻ 683.2901, obsd 683.2888.

1-(β-D-Ribofuranosyl)-5'-O-(4,4'-dimethoxytrityl)-2'-O-(t-butyl dimethylsilyl)-3'-O-(2-cyanoethyl N,N-diisopropylphosphoramidite)-1H-pyrazolo[3,4-d]pyrimidin-4(5H)-one(6): Compound (**5**) (0.4 g, 0.585 mmol) was dried *in vacuo* overnight. Anhydrous dichloromethane (5 mL) and freshly distilled DIPEA (590 μL, 3.51 mmol) were added to the flask. To the solution was added (2-cyanoethyl)-N,N-diisopropylchlorophosphoramidite (389.5 μL, 1.75 mmol), and the mixture was stirred at room temperature for 4 h. The reaction mixture was quenched with anhydrous methanol. Immediately, the mixture was extracted with saturated aqueous NaHCO₃ (10 mL) and EtOAc (20 mL). The organic phases were washed with brine (15 mL) and dried over Na₂SO₄. The solvent was removed under reduced pressure. The residue was purified by column chromatography on silica gel with hexane/EtOAc (1:1) to give (**6**) (401 mg, 77%) as a white foam. ³¹P NMR (CD₂Cl₂, 252.5MHz): δ (ppm) 150.52, 148.84.

ESIHRMS (m/z): calcd for C₄₆H₆₀N₆O₈PSi [M-H]⁻ 883.3977, obsd 883.3981.

1.3 RNA synthesis and analysis—7d8aI-containing oligos were synthesized at the University of Utah DNA/Peptide Core Facility using the 7-deaza-8-azainosine

phosphoramidite on a 1 μ mol scale. Mass spectrometry data was acquired using a Bruker UltraFlex extreme MALDI-TOF/TOF. Identity of the oligonucleotide containing the 7-deaza-8-azainosine was confirmed by MALDI-TOF mass spectroscopy using a saturated solution of 3-hydroxypicolinic acid in 0.1 M aqueous dibasic ammonium citrate as a matrix. Mass spectra were recorded in the negative ionization mode and calibrated to an external DNA standard of 7143.59 Daltons. Samples and standards were further desalted using EMD Millipore micro ziptips for MALDI-TOF sample preparation. 7d8aI5 20 mer: [M-H]⁻-calcd. 6175.6 obsd. 6173.9; 7d8aI modified 12 mer: [M-H]⁻-calcd. 3852.3 obsd. 3856.1

2. HEK293-TLR8 cell assay

2.1 Sample preparation—All RNAs in TLR8 agonist experiments were incubated at a final concentration of 5 μ M in DMEM, with DOTAP (200 U per nmol RNA). In TLR8 antagonist experiments using c7G5 against R848, c7G5 was incubated with 3 μ g/ml R848 in DMEM and DOTAP (200 U per nmol RNA). In all other TLR8 antagonist experiments, antagonist strands were incubated with 5 μ M of G5 in DMEM, with DOTAP (200 U per nmol RNA).

2.2 Cell culture and TLR8 activity assay—HEK293-TLR8 cells were grown in Dulbecco's modified Eagle's medium (DMEM, GIBCO), supplemented with 1 x penicillin-streptomycin (Pen-Strep; Gibco) and 10 % fetal bovine serum, and incubated in 5 % CO₂ at 37 °C. Cells were allowed to grow in flasks until they reached 80–90 % confluence, then treated with Accutase (Innovative Cell Technologies) and diluted in fresh DMEM (10 % FBS, 1 x Pen–Strep) to a concentration of 1 x 10⁵ cells/mL.

Cells were plated in a 96 well plate with 1 x 10⁵ cells/ml in DMEM medium and 10% fetal bovine serum without Pen-Strep, 24 h before samples were added. The samples were prepared by mixing RNA and DOTAP (200 U per nmol RNA) and incubating at room temperature for 30 min. Then the culture medium was replaced by different samples at 100 μ L per well, each condition carried out in triplicate. After incubating for another 24 h, the concentration of Secreted Alkaline Phosphatase was determined with Secreted Alkaline Phosphatase Reporter Assay Kit (Novusbio Inc.). The activity of TLR8 was then normalized by setting the SEAP concentration of cells treated with only DOTAP as 0, while SEAP concentration of cells treated with 5 μ M of G5 as 1.

3. Cell toxicity assay

Cell toxicity for the samples used in TLR8 assays was determined to rule out possible effect of cell toxicity on SEAP concentration. Cells were cultured under the same conditions as in the TLR8 assay, and samples with or without G5 were prepared and transfected in the same way as in the TLR8 assay. After incubation, the toxicity of each sample is determined by CellToxTM Green Cytotoxicity Assay Kit. The relative toxicity is plotted by setting the toxicity of untreated cells as 0 and the toxicity of cells treated with cell lysis (provided within CellToxTM Green Cytotoxicity Assay Kit, 4 μ L per well) as 1. No significant toxicity was observed under the experimental conditions (Figure S1).

4. Tm analysis

The thermal stability of the guanosine, inosine and 7d8aI containing RNAs were analyzed in a 12 bp duplex of sequence using a procedure previously described²⁷ and the following buffer conditions: 10 mM Tris-HCl, pH 7.8, 0.1 mM EDTA and 100 mM NaCl. The values reported in Figure S2 are an average of three denaturation experiments, with the experimental temperature range noted for each RNA duplex.

Supplementary Material

Refer to Web version on PubMed Central for supplementary material.

Acknowledgments

This work was supported by a grant to PAB from the National Institutes of Health (USA) (R01 GM080784).

References and notes

1. Shizuo A, Takeda K, Kaisho T. Toll-like receptors: critical proteins linking innate and acquired immunity. *Nat Immunol.* 2001; 2(8):675–680. [PubMed: 11477402]
2. Marshak-Rothstein A. Toll-like receptors in systemic autoimmune disease. *Nat Rev Immunol.* 2006; 6(11):823–835. [PubMed: 17063184]
3. Heidegger S, van den Brink MRM, Haas T, Poeck H. The Role of Pattern-Recognition Receptors in Graft-Versus-Host Disease and Graft-Versus-Leukemia after Allogeneic Stem Cell Transplantation. *Front Immunol.* 2014; 5:337. [PubMed: 25101080]
4. Bessis N, GarciaCozar FJ, Boissier MC. Immune responses to gene therapy vectors: influence on vector function and effector mechanisms. *Gene Ther.* 2004; 11(S1):S10–17. [PubMed: 15454952]
5. Finberg RW, Wang JP, Kurt-Jones EA. Toll like receptors and viruses. *Rev Med Virol.* 2007; 17(1): 35–43. [PubMed: 17146842]
6. Kawai T, Akira S. TLR signaling. *Cell Death Differ.* 2006; 13(5):816–825. [PubMed: 16410796]
7. Guiducci C, Gong M, Cepika A-M, et al. RNA recognition by human TLR8 can lead to autoimmune inflammation. *J Exp Med.* 2013; 210(13):2903. [PubMed: 24277153]
8. Clancy RM, Alvarez D, Komissarova E, Barrat FJ, Swartz J, Buyon JP. Ro60-associated single-stranded RNA links inflammation with fetal cardiac fibrosis via ligation of TLRs: a novel pathway to autoimmune-associated heart block. *J Immunol.* 2010; 184(4):2148–2155. [PubMed: 20089705]
9. Tanji H, Ohto U, Shibata T, et al. Toll-like receptor 8 senses degradation products of single-stranded RNA. *Nat Struct Mol Biol.* 2015; 22(2):109–115. [PubMed: 25599397]
10. Tanji H, Ohto U, Shibata T, Miyake K, Shimizu T. Structural Reorganization of the Toll-Like Receptor 8 Dimer Induced by Agonistic Ligands. *Science.* 2013; 339(6126):1426. [PubMed: 23520111]
11. Peacock H, Fucini RV, Jayalath P, et al. Nucleobase and Ribose Modifications Control Immunostimulation by a MicroRNA-122-mimetic RNA. *J Am Chem Soc.* 2011; 133(24):9200–9203. [PubMed: 21612237]
12. Valenzuela RAP, Suter SR, Ball-Jones AA, Ibarra-Soza JM, Zheng Y, Beal PA. Base Modification Strategies to Modulate Immune Stimulation by an siRNA. *ChemBioChem.* 2015; 16(2):262–267. [PubMed: 25487859]
13. Sioud M, Furset G, Cekaite L. Suppression of immunostimulatory siRNA-driven innate immune activation by 2'-modified RNAs. *Biochem Biophys Res Commun.* 2007; 361(1):122–126. [PubMed: 17658482]
14. Lan T, Kandimalla ER, Yu D, et al. Stabilized immune modulatory RNA compounds as agonists of Toll-like receptors 7 and 8. *Proc Natl Acad Sci U S A.* 2007; 104(34):13750–13755. [PubMed: 17698957]

15. Sarvestani ST, Tate MD, Moffat JM, et al. Inosine-Mediated Modulation of RNA Sensing by Toll-Like Receptor 7 (TLR7) and TLR8. *J Virol*. 2014; 88(2):799–810. [PubMed: 24227841]
16. Hougland JL, Deb SK, Maric D, Piccirilli JA. An Atomic Mutation Cycle for Exploring RNA's 2'-Hydroxyl Group. *J Am Chem Soc*. 2004; 126(42):13578–13579. [PubMed: 15493890]
17. Krüger A, Oldenburg M, Chebroly C, et al. Human TLR8 senses UR/URR motifs in bacterial and mitochondrial RNA. *EMBO Rep*. 2015; 16(12):1656. [PubMed: 26545385]
18. Vollmer J, Tluk S, Schmitz C, et al. Immune stimulation mediated by autoantigen binding sites within small nuclear RNAs involves Toll-like receptors 7 and 8. *J Exp Med*. 2005; 202(11):1575. [PubMed: 16330816]
19. Sioud M. Induction of Inflammatory Cytokines and Interferon Responses by Double-stranded and Single-stranded siRNAs is Sequence-dependent and Requires Endosomal Localization. *J Mol Biol*. 2005; 348(5):1079–1090. [PubMed: 15854645]
20. Rimbach K, Kaiser S, Helm M, Dalpke AH, Eigenbrod T. 2'-O-Methylation within Bacterial RNA Acts as Suppressor of TLR7/TLR8 Activation in Human Innate Immune Cells. *J Innate Immun*. 2015; 7(5):482–493. [PubMed: 25823462]
21. Schmitt FCF, Freund I, Weigand MA, Helm M, Dalpke AH, Eigenbrod T. Identification of an optimized 2'-O-methylated tri-nucleotide RNA motif inhibiting Toll-like receptor 7 and 8. *RNA*. 2017
22. Schlee M, Hornung V, Hartmann G. siRNA and isRNA: two edges of one sword. *Mol Ther*. 14(4): 463–470.
23. Judge A, MacLachlan I. Overcoming the Innate Immune Response to Small Interfering RNA. *Hum Gene Ther*. 2008; 19(2):111–124. [PubMed: 18230025]
24. Trieu A, Bokil N, Dunn JA, et al. TLR9-independent effects of inhibitory oligonucleotides on macrophage responses to *S. typhimurium*. *Immunol Cell Biol*. 2008; 87(3):218–225. [PubMed: 19048019]
25. Lin W, Li H, Ming X, Seela F. 1,N6-Etheno-7-deaza-2,8-diazaadenosine: syntheses, properties and conversion to 7-deaza-2,8-diazaadenosine. *Org Biomol Chem*. 2005; 3(9):1714–1718. [PubMed: 15858655]
26. Agarwal RP, Sagar SM, Parks RE. Adenosine deaminase from human erythrocytes: Purification and effects of adenosine analogs. *Biochem Pharmacol*. 1975; 24(6):693–701. [PubMed: 1125070]
27. Peacock H, Maydanovych O, Beal PA. N2-Modified 2-aminopurine ribonucleosides as minor-groove-modulating adenosine replacements in duplex RNA. *Org Lett*. 2010; 12(5):1044–1047. [PubMed: 20108910]

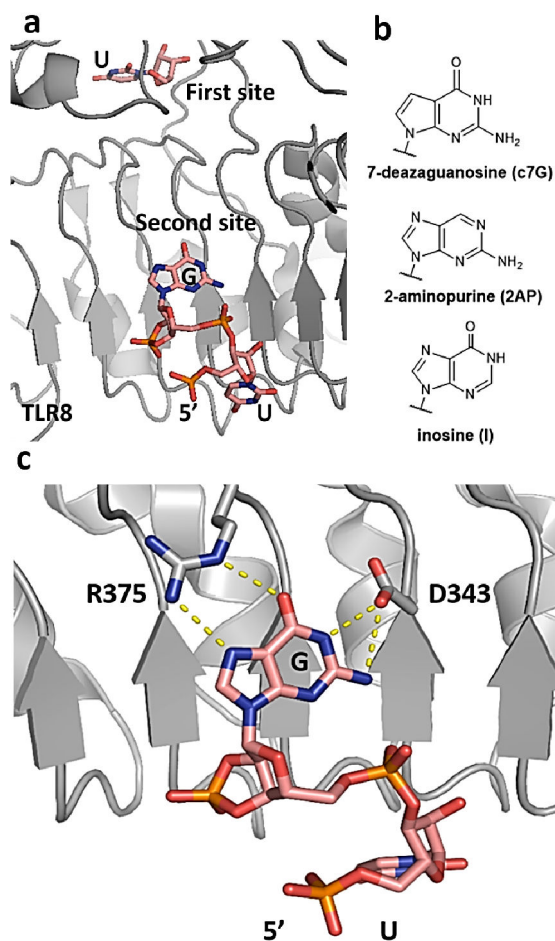


Figure 1.
a: X-ray crystal structure of TLR8 binding with ssRNA degradation products in two binding sites; **b:** Guanosine modifications used in the study; **c:** Close up view of UpG binding with TLR8 in the second binding site.

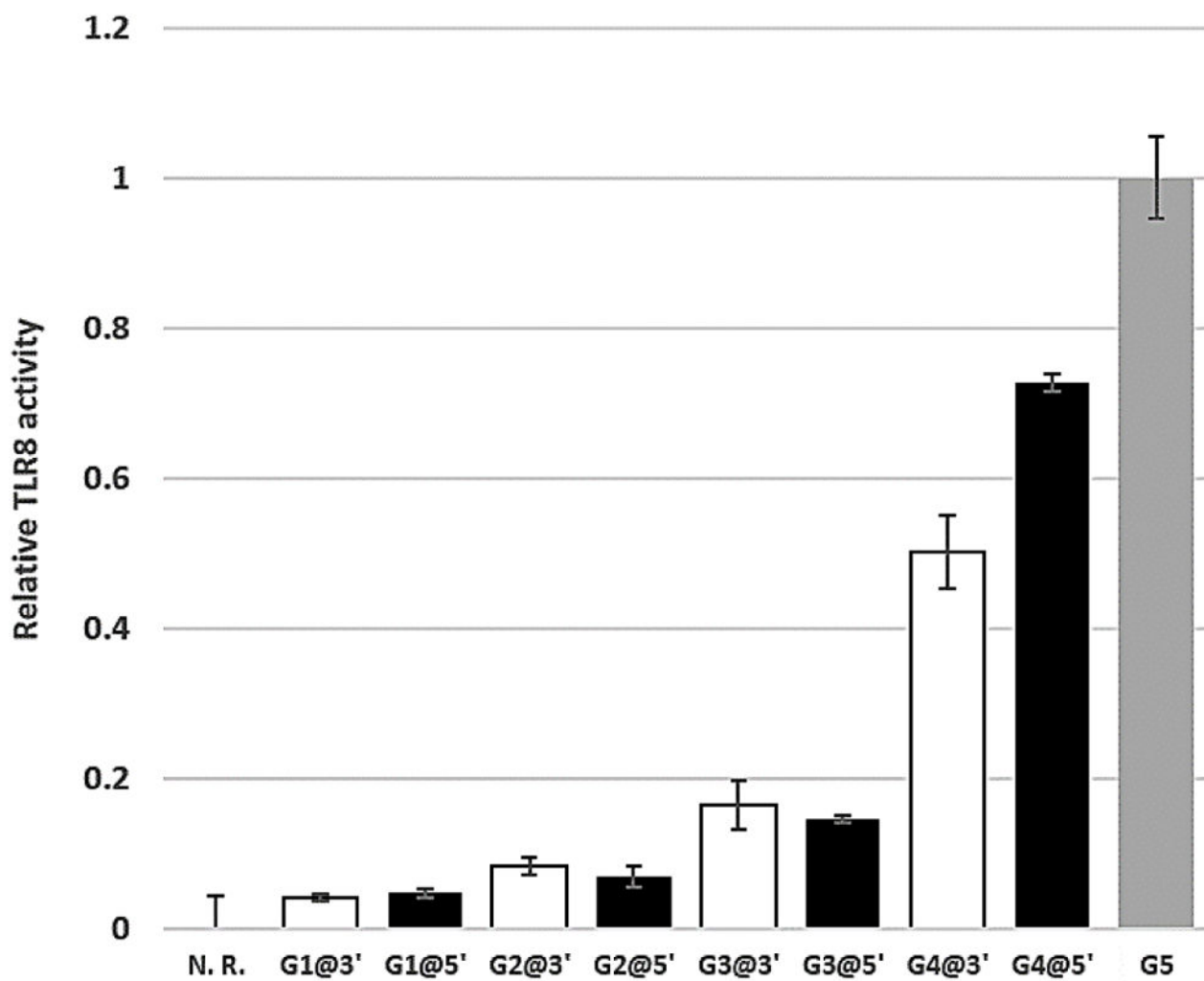


Figure 2. Activity of ssRNA on TLR8 stimulation increases with the number of UpG motifs present. The TLR8 activity of G5 was normalized to 1, while the TLR8 activity without RNA (N. R.) has been set as 0. White: G on 3'; Black: G on 5'. All oligos were tested at 5 μ M on HEK293-TLR8 cells, transfected with DOTAP

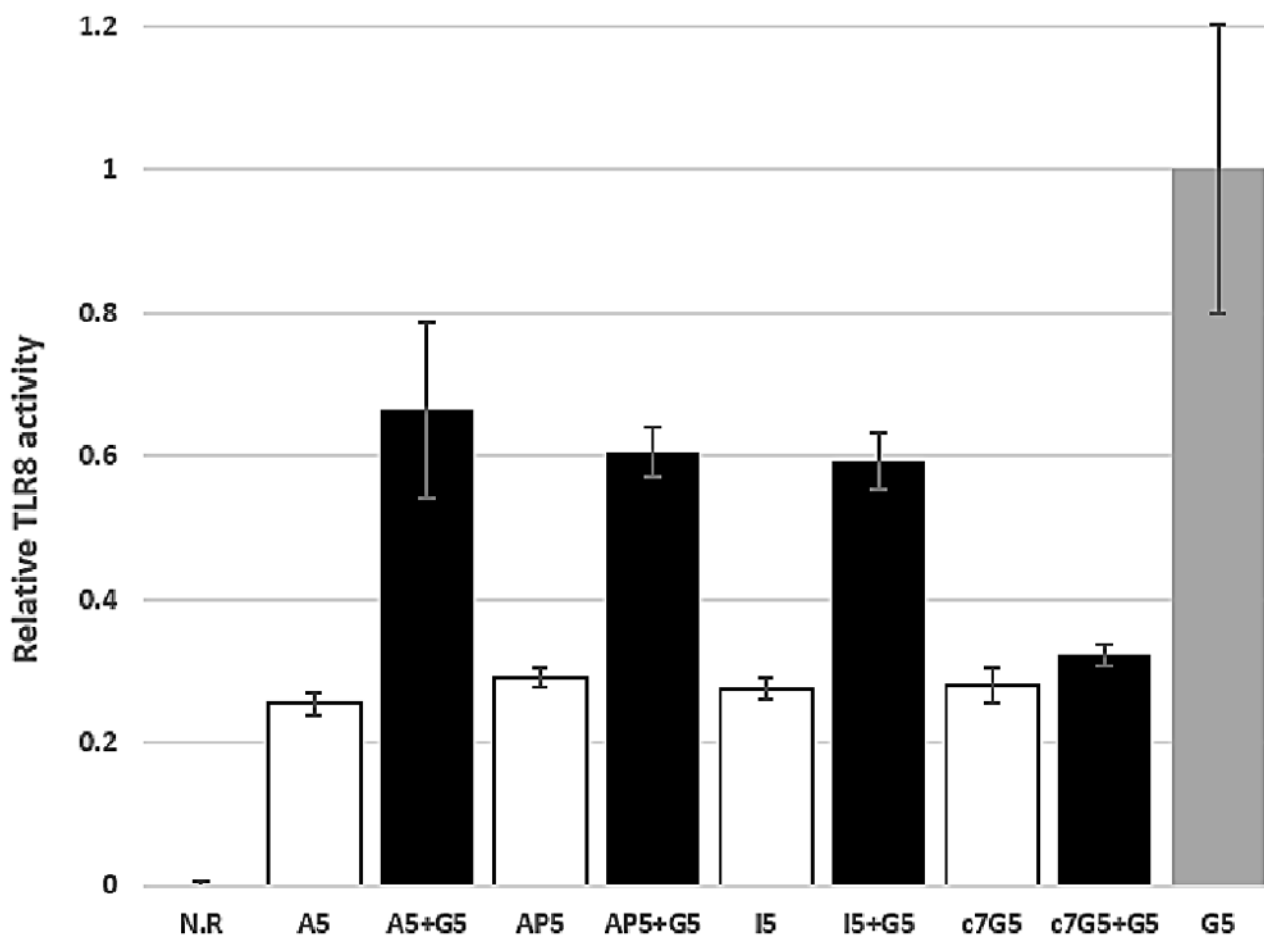


Figure 3. Agonistic and antagonistic effect of different guanosine modifications on TLR8. All oligos were transfected by DOTAP at 5 μ M. White: Agonism; Black: Antagonism

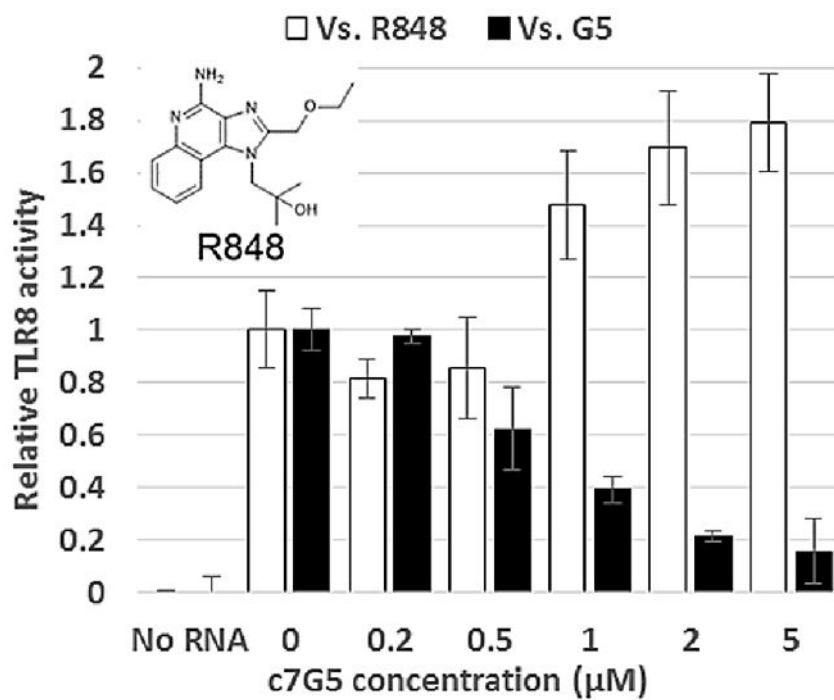


Figure 4. c7G5 antagonizes G5 but not R848. c7G5 co-incubated with 5μM of UG5 or 3μg/ml R848, transfected with DOTAP.

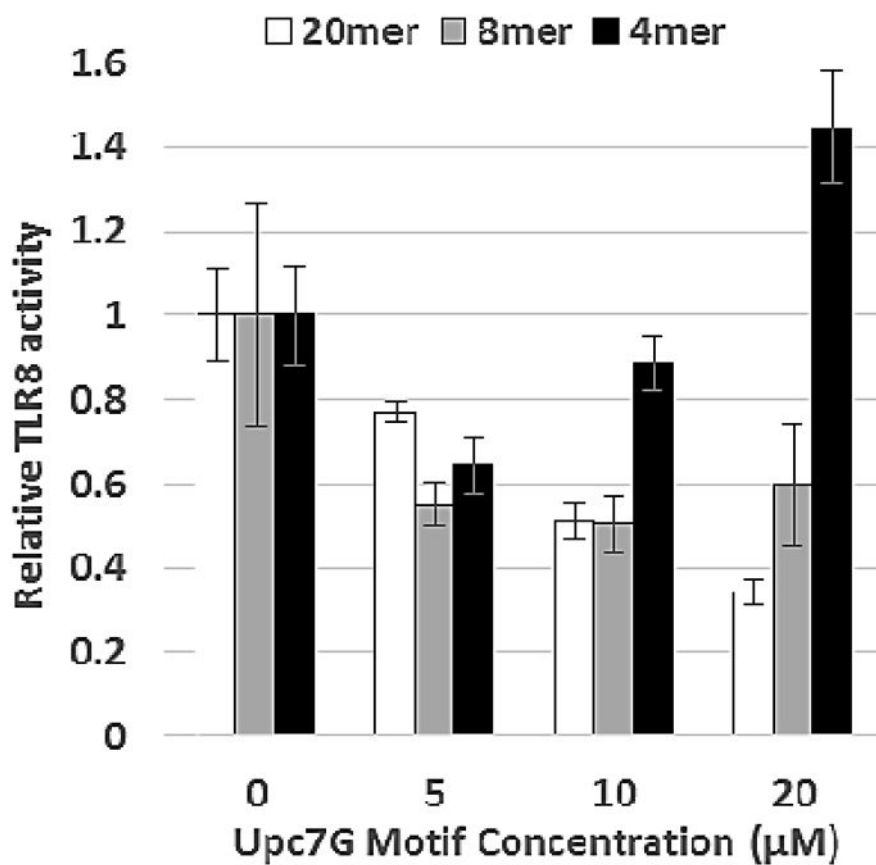


Figure 5. The antagonism of longer ssRNA is stronger, especially under higher concentrations. All oligos were co-incubated with G5 and transfected with DOTAP

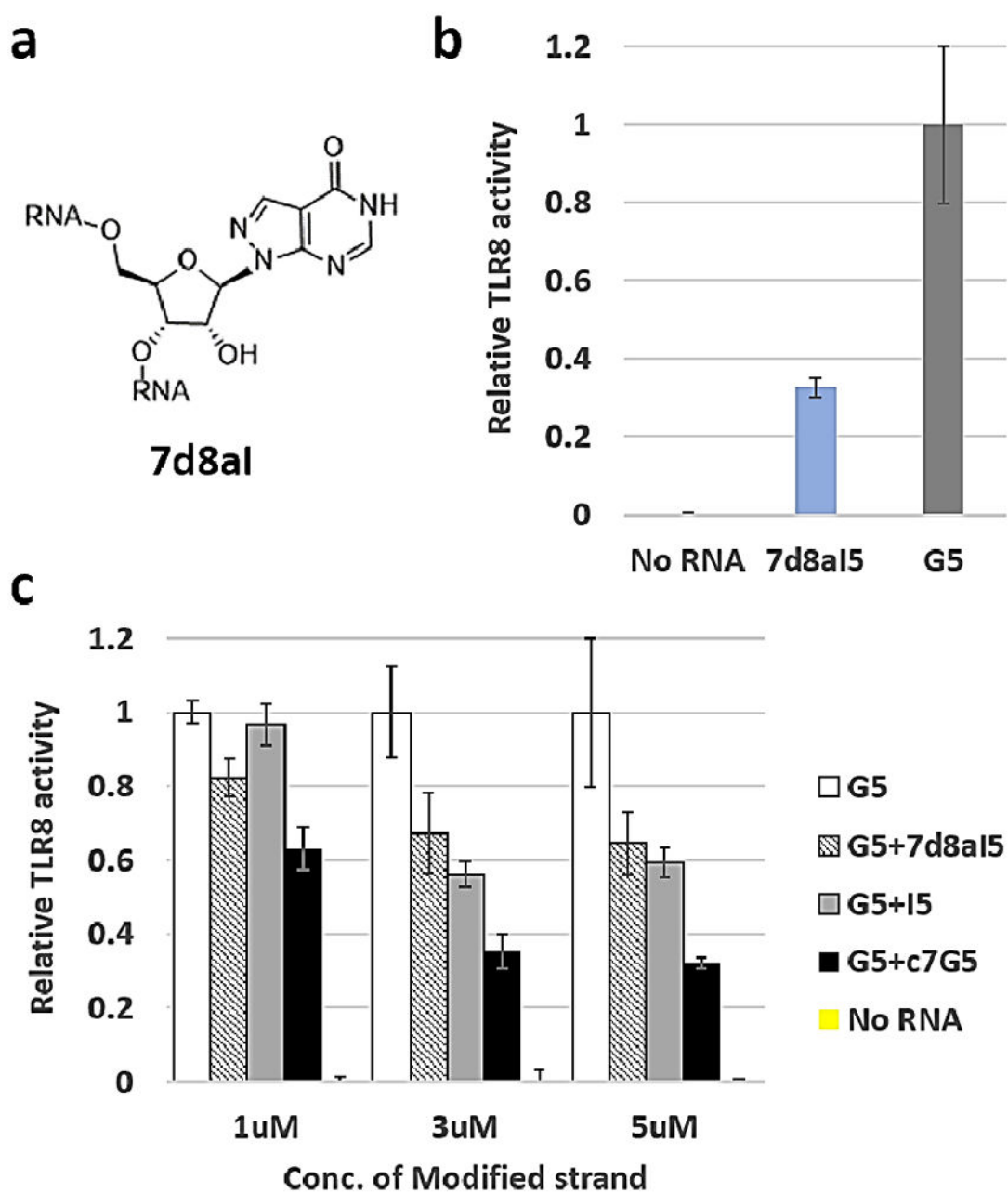


Figure 6.

a. Chemical structure of 7d8aI in RNA; **b.** Agonistic activity of 7d8aI5 is lower than G5, both transfected with DOTAP at 5 μ M; **c.** 7d8aI5 has similar antagonism against G5 as I5, while c7G5 is a stronger antagonist.

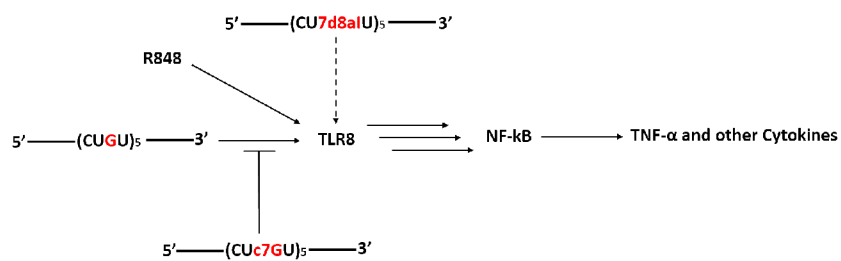
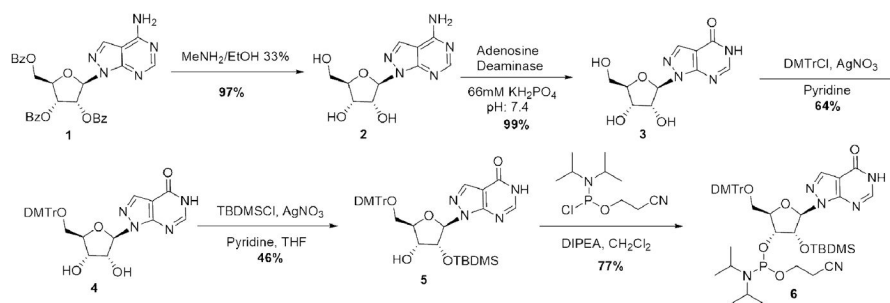


Figure 7. Pathway of TLR8 activation and antagonism by ssRNAs containing different guanosine analogs. Arrows: activation; T-shaped arrow: antagonism; Dash arrow: weak interaction; c7G: 7-deazaguanosine; 7d8aI: 7-deaza-8-azainosine.



Scheme 1.
Synthesis route of 7d8aI phosphoramidite

Table 1

Sequences and abbreviations for the ssRNAs used in the study. AP, 2-aminopurine; I, inosine; c7G, 7-deazaguanosine; 7d8aI, 7-deaza-8-azainosine

Name	Sequence
G5	5'-CUGUCUGUCUGUCUGUCUGU-3'
G1@3'	5'-CUCUCUCUCUCUCUCUCUGU-3'
G1@5'	5'-CUGUCUCUCUCUCUCUCUCU-3'
G2@3'	5'-CUCUCUCUCUCUCUGUCUGU-3'
G2@5'	5'-CUGUCUGUCUCUCUCUCUCU-3'
G3@3'	5'-CUCUCUCUCUGUCUGUCUGU-3'
G3@5'	5'-CUGUCUGUCUGUCUCUCUCU-3'
G4@3'	5'-CUCUCUGUCUGUCUGUCUGU-3'
G4@5'	5'-CUGUCUGUCUGUCUGUCUCU-3'
AP5	5'-CUAPUCUAPUCUAPUCUAPUCUAPU-3'
I5	5'-CUIUCUIUCUIUCUIUCUIU-3'
c7G5	5'-CUc7GUCUc7GUCUc7GUCUc7GUCUc7GU-3'
7d8aI5	5'-CU7d8aIUCU7d8aIUCU7d8aIUCU7d8aIUCU7d8aIU-3'
A5	5'-CUAUCUAUCUAUCUAUCUAU-3'
8-mer Uc7G	5'-CUc7GUCUc7GU-3'
4-mer Uc7G	5'-CUc7GU-3'